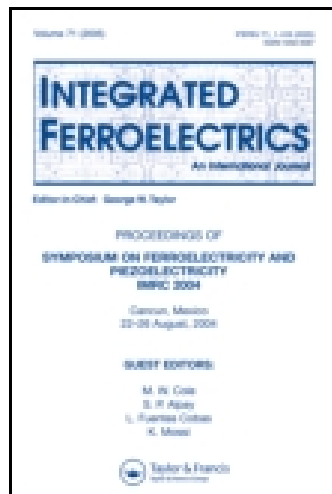


This article was downloaded by: [49.48.116.23]

On: 24 June 2014, At: 22:50

Publisher: Taylor & Francis

Informa Ltd Registered in England and Wales Registered Number: 1072954 Registered office: Mortimer House, 37-41 Mortimer Street, London W1T 3JH, UK



## Integrated Ferroelectrics: An International Journal

Publication details, including instructions for authors and subscription information:

<http://www.tandfonline.com/loi/ginf20>

### Numerical Simulation of n-CaMnO<sub>3</sub>/Bi and p-NaCo<sub>2</sub>O<sub>4</sub>/Ag Thermoelectric Cell by Finite Element Method

Suriya Srichai<sup>a</sup> & Tosawat Seetawan<sup>a</sup>

<sup>a</sup> Thermoelectrics Research Center and Program of Physics, Faculty of Science and Technology, Sakon Nakhon Rajabhat University, 680 Nittayo Rd., Sakon Nakhon 47000, Thailand

Published online: 20 Jun 2014.

To cite this article: Suriya Srichai & Tosawat Seetawan (2014) Numerical Simulation of n-CaMnO<sub>3</sub>/Bi and p-NaCo<sub>2</sub>O<sub>4</sub>/Ag Thermoelectric Cell by Finite Element Method, Integrated Ferroelectrics: An International Journal, 156:1, 6-14, DOI: [10.1080/10584587.2014.906181](https://doi.org/10.1080/10584587.2014.906181)

To link to this article: <http://dx.doi.org/10.1080/10584587.2014.906181>

PLEASE SCROLL DOWN FOR ARTICLE

Taylor & Francis makes every effort to ensure the accuracy of all the information (the "Content") contained in the publications on our platform. However, Taylor & Francis, our agents, and our licensors make no representations or warranties whatsoever as to the accuracy, completeness, or suitability for any purpose of the Content. Any opinions and views expressed in this publication are the opinions and views of the authors, and are not the views of or endorsed by Taylor & Francis. The accuracy of the Content should not be relied upon and should be independently verified with primary sources of information. Taylor and Francis shall not be liable for any losses, actions, claims, proceedings, demands, costs, expenses, damages, and other liabilities whatsoever or howsoever caused arising directly or indirectly in connection with, in relation to or arising out of the use of the Content.

This article may be used for research, teaching, and private study purposes. Any substantial or systematic reproduction, redistribution, reselling, loan, sub-licensing, systematic supply, or distribution in any form to anyone is expressly forbidden. Terms & Conditions of access and use can be found at <http://www.tandfonline.com/page/terms-and-conditions>

# Numerical Simulation of n-CaMnO<sub>3</sub>/Bi and p-NaCo<sub>2</sub>O<sub>4</sub>/Ag Thermoelectric Cell by Finite Element Method

SURIYA SRICHAI AND TOSAWAT SEETAWAN\*

Thermoelectrics Research Center and Program of Physics, Faculty of Science  
and Technology, Sakon Nakhon Rajabhat University, 680 Nittayo Rd., Sakon  
Nakhon 47000, Thailand

*In the optimal design of thermoelectric cell, the electrical power, voltage and efficiency are interesting issues to investigate. We simulated thermoelectric cells to study the distribution temperature, voltage, current, electric power and efficiency by finite element method (FEM). The elements were used Brick 20 node 226 and tetrahedron 227 from the mesh tools element attributes mesh volume p-n type for hexagonal and copper for tetrahedron boundary condition to the thermoelectric cell. The calcium bismuth manganese oxide n-type (CaMnO<sub>3</sub>/Bi) leg and sodium cobalt oxide doping silver p-type (NaCo<sub>2</sub>O<sub>4</sub>/Ag) leg size of 2.5×2.5×10 mm<sup>3</sup> was fabricated in FEM. copper plate size of 2.5×5.5×0.5 mm<sup>3</sup>. The electrical resistance of 17 Ω, voltage of 0.96 V, current of 3.68 mA, electric power of 3.53 mW and conversion efficiency of 1.76 % at temperature difference of 200 K.*

**Keywords** Numerical simulation; finite element method and thermoelectric generator

## 1. Introduction

Thermoelectric devices are solid state electric generators with no moving parts, when subject to a temperature gradient across their ends produce an electromotive force (emf). Efficient TE materials are characterized by a high thermoelectric figure of merit  $ZT (\approx 1)$ , where  $ZT = S^2 \sigma T / \kappa$ ,  $T$  is absolute temperature (K),  $S$  is Seebeck coefficient,  $\sigma$  is electrical conductivity, and  $\kappa$  is thermal conductivity. Advantages such as the high degree of reliability, simplicity, tacit operation, lack of vibrations, and scalability render Thermoelectric Generators (TEGs) ideal for small scale, distribution of power generation, and energy harvesting applications [1]. To answer these needs, the thermoelectric analysis has been performed in ANSYS 13.0 [2]. The ANSYS finite element program has a large library of elements that supports structural, thermal, fluid, acoustic, and electromagnetic analyses. The coupled-field elements that simulate the interaction between the above fields are also examples of ANSYS. This research focuses on the numerical simulation of 1&17 cells with ANSYS. We simulated thermoelectric cell to study the distribution temperature, voltage, current, electric power and efficiency by Finite Element Method (FEM).

---

Received July 23, 2013; in final form January 12, 2014.

\*Corresponding author. E-mail: t.seetawan@snru.ac.th; suriya.07@hotmail.com

Color versions of one or more of the figures in the article can be found online at [www.tandfonline.com/ginf](http://www.tandfonline.com/ginf).

## 2. Equations of Thermoelectricity

$$\rho C \frac{\partial T}{\partial t} + \vec{\nabla} \cdot \vec{q} = \dot{q} \quad (1)$$

and of continuity of electric charge

$$\vec{\nabla} \cdot \left( \vec{J} + \frac{\partial \vec{D}}{\partial t} \right) = 0 \quad (2)$$

and coupled by the set of thermoelectric constitutive equations [3].

$$\vec{q} = [\Pi] \cdot \vec{J} - [\kappa] \cdot \vec{\nabla} T, \quad (3)$$

$$\vec{J} = [\sigma] \cdot \left( \vec{E} - [S] \cdot \vec{\nabla} T \right) \quad (4)$$

and the constitutive equation for a dielectric medium

$$\vec{D} = [\varepsilon] \cdot \vec{E}, \quad (5)$$

where:

$\rho$  = density, kg/m<sup>3</sup>,

$C$  = specific heat capacity, J/ kg K,

$T$  = absolute temperature, K,

$\dot{q}$  = heat generation rate per unit volume, W/m<sup>3</sup>,

$\vec{q}$  = heat flux vector, W/m<sup>2</sup>,

$\vec{J}$  = electric current density vector, A/m<sup>2</sup>,

$\vec{E}$  = electric field intensity vector, V/m,

$\vec{D}$  = electric flux density vector, C/m<sup>2</sup>,

$[\kappa]$  = thermal conductivity matrix, W/m K,

$[\sigma]$  = electrical conductivity matrix, S/m,

$[S]$  = Seebeck coefficient matrix, V/K,

$[\Pi]$  = Peltier coefficient matrix, V,

$[\varepsilon]$  = dielectric permittivity matrix, F/m.

Output power and thermal flux of TEG

$$Q_h = ST_h I - \frac{1}{2} I^2 R_0 + \kappa \Delta T \text{ and } q_h = \frac{Q_h}{A_h} \quad (6)$$

where  $A_h$  stands for the hot-side area of TEG model [4].



The output power is defined as follows:

$$P = I^2 R_L \quad (7)$$

where  $I$  and  $R_L$  electric current and load resistance, respectively. Generally, when output power is maximum, electric resistance is equal to the internal resistance of TEG. And the current can be calculated as

$$I = \frac{S \Delta T}{R_0 + R_L} \quad (8)$$

**Table 1**  
Finite elements for a thermoelectric  
analysis

SOLID226		3-D 20-node hexahedron
SOLID227		3-D 10-node tetrahedron

where  $R_0$  is the generator resistance. So the thermal input  $Q_h$  and thermal flux  $q_h$  to the hot side are obtained by

$$\eta_{TEG} = \frac{P_{out}}{Q_{in}} \tag{9}$$

where  $Q_{in}$  stands for input power. The total efficiency of thermoelectric generator is the product of the thermoelectric conversion efficiency  $\eta_{TEG}$  [5–7].

**3. Finite Element Formulation**

The global matrix equation is assembled from the individual finite element equations [8]. Since the thermal load vector or element matrixes depends on the electric solution, the analysis is non-linear (steady-state or time-transient) and requires at least two iterations to converge. As shown in Table 1, the mesh conditions of thermoelectric materials is solid 226 and copper is solid 227 because copper strips are thin.

*Numerical Simulation of TEG*

The thermoelectric is a major component which can utilize waste heat to produce auxiliary thermoelectric conversion. The design can effectively improve the performance of TEG at mentioned above. The distribution of heat flux on TEG under different operating conditions has also been obtained using ANSYS. The material properties such as Seebeck coefficient, thermal conductivity and resistivity are summarized in Table 2.

**Table 2**  
Thermoelectric properties of sodium cobalt oxide doping silver ( $\text{NaCo}_2\text{O}_4/\text{Ag}$ ) and calcium bismuth manganese oxide ( $\text{CaMnO}_3/\text{Bi}$ ) based on finite element method analysis.

Materials	Seebeck coefficient ( $\mu\text{V}/\text{K}^{-1}$ )	Resistivity ( $\Omega\cdot\text{m}$ )	Thermal conductivity ( $\text{Wm}^{-1}\text{K}^{-1}$ )
$\text{NaCo}_2\text{O}_4/\text{Ag}$	122	$1.32 \times 10^{-4}$	2.5
$\text{CaMnO}_3/\text{Bi}$	–148	$4.02 \times 10^{-4}$	1
Copper	6.5	$5.9 \times 10^{-8}$	350
$\text{Al}_2\text{O}_3$	–	$10^{14}$	40

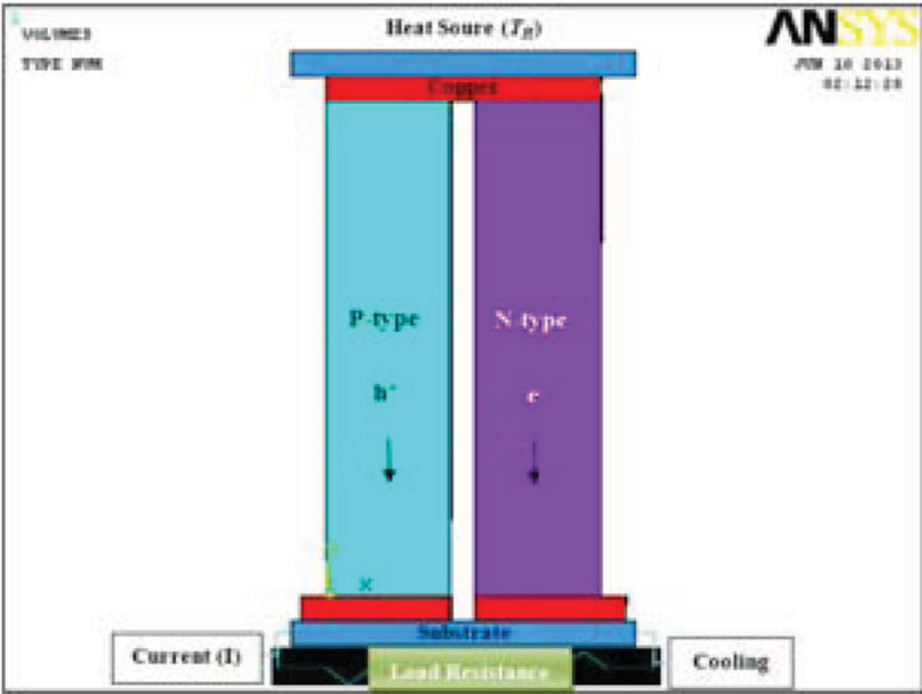


Figure 1. Boundary condition for the thermoelectric cell.

4. Materials and Methods

Sample Preparation

We prepared thermoelectric p-type sodium cobalt oxide doping silver ( $\text{NaCo}_2\text{O}_4/\text{Ag}$ ) and the n-type calcium bismuth manganese oxide ( $\text{CaMnO}_3/\text{Bi}$ ) material for thermoelectric measurement of the properties as shown in Table 2. The distributions of voltage and under differential operating conditions and distributions of temperatures for thermoelectric cell

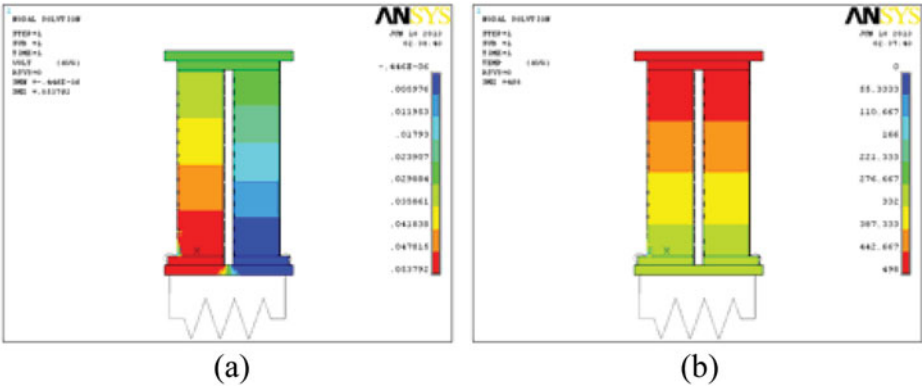
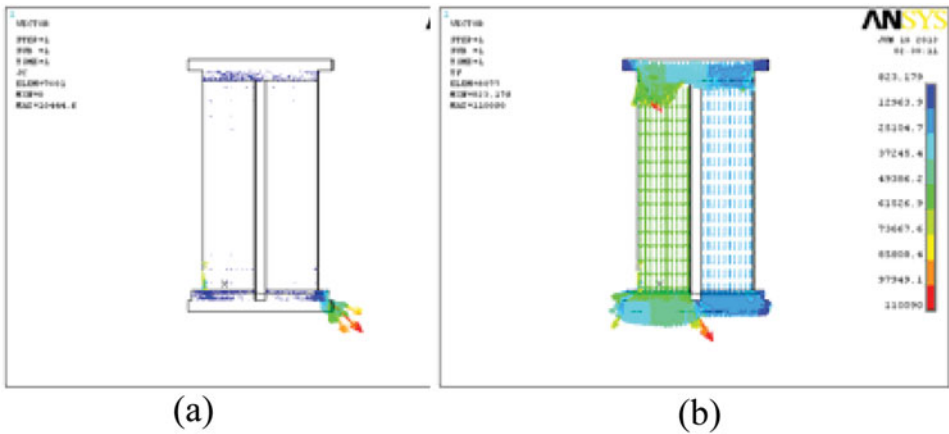


Figure 2. (a) Distributions of voltage for thermoelectric FEM cell under differential operating conditions and (b) distributions of temperatures for thermoelectric cell on FEM.



**Figure 3.** (a) Direction current density and (b) distributions of heat flux per cross-sectional area on TEG.

on FEM as shown in Fig. 2. The direction current density and distributions of heat flux per cross-sectional area on TEG as shown in Fig. 3.

**5. Results and Discussion**

Numerical simulation was carried out by using finite element method, design of thermo-electric cell, the electrical power, voltage and efficiency. Apply boundary conditions and

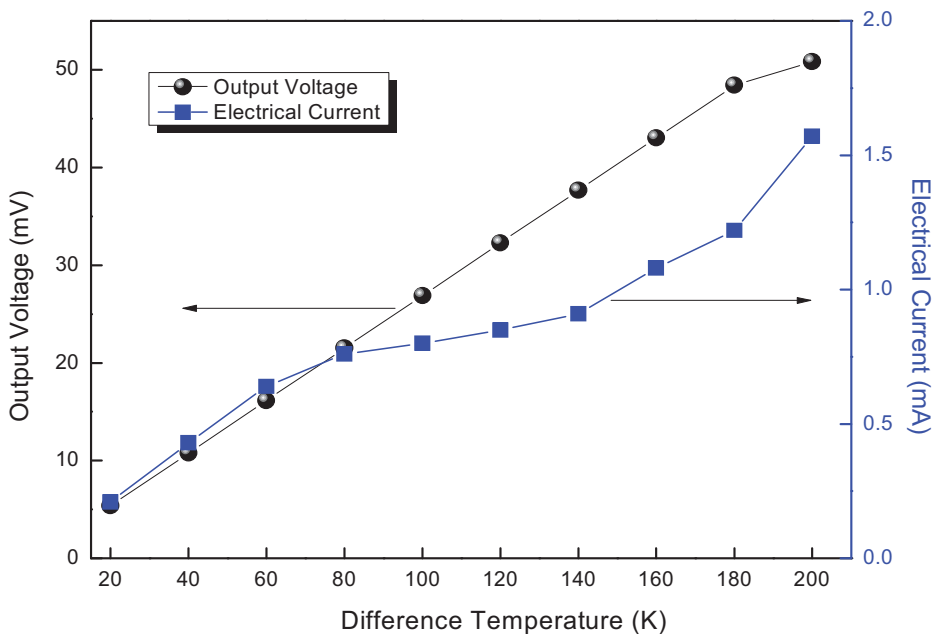


**Figure 4.** The result of numerical simulation of voltage, electrical current at difference temperature ranging from 20–200 K.

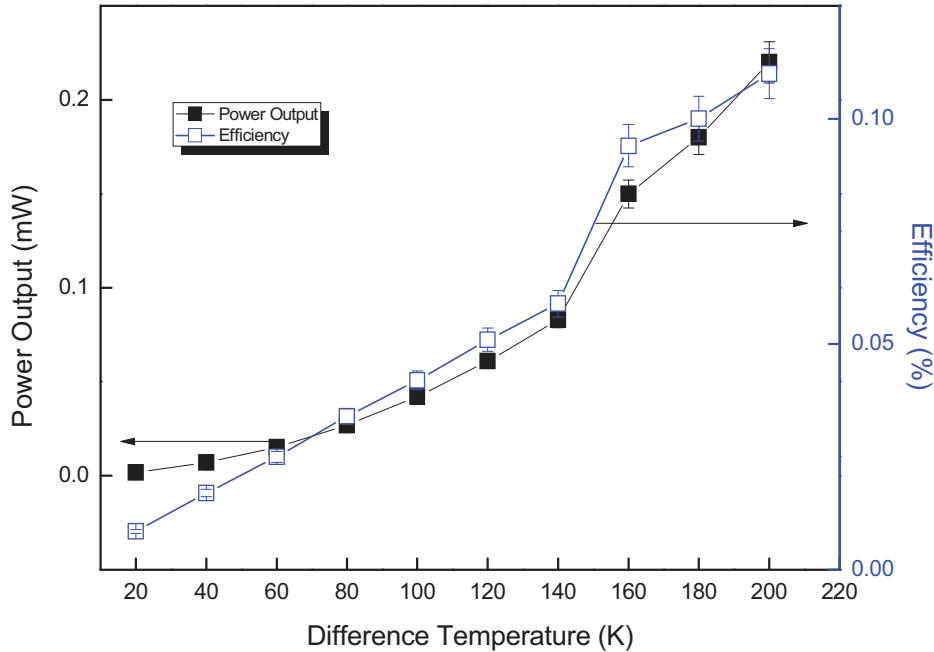


**Figure 5.** The result of numerical simulation of power output, efficiency at difference temperature ranging from 20–200 K.

loads excitation were set of p-type electrode voltage at zero condition and range temperature obtain the solution result as shown in Fig. 1.

The thermoelectric generator was obtained numerical simulation for 1 and 17 cells.

Figure 4 shows the voltage and electrical current produced by TEG cell rise sharply to the maximum of 50.82 mV and 1.57 mA, respectively, which is obtained from the generation characteristic of TEG. Fig. 5 shows the power output and efficiency each cell rise with increasing difference temperature at 200 K, power and efficiency is 0.11 % output

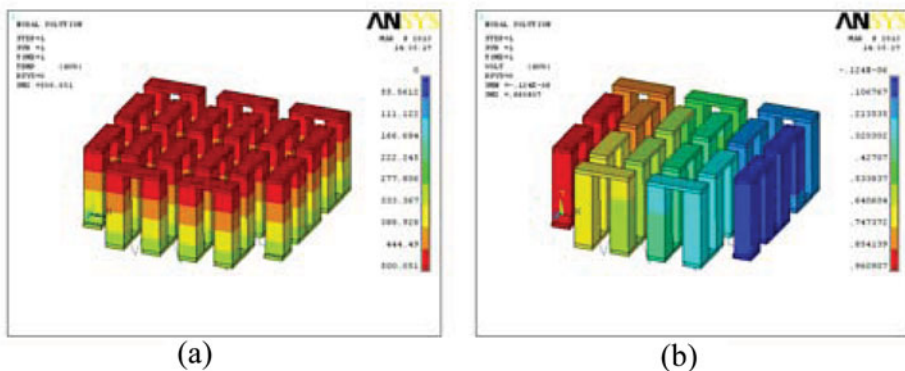


**Figure 6.** (a) Distributions of temperatures for thermoelectric on FEM 17 cell and (b) distributions of voltage for thermoelectric FEM cell under different operating conditions.

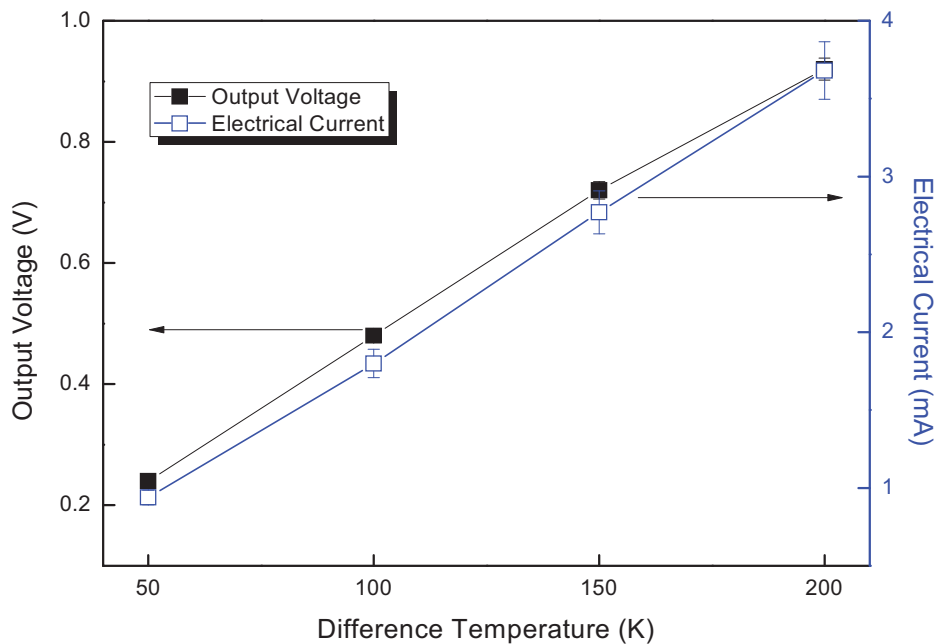


**Figure 7.** The result of numerical simulation of voltage, electrical current at difference temperature ranging from 50–200 K.

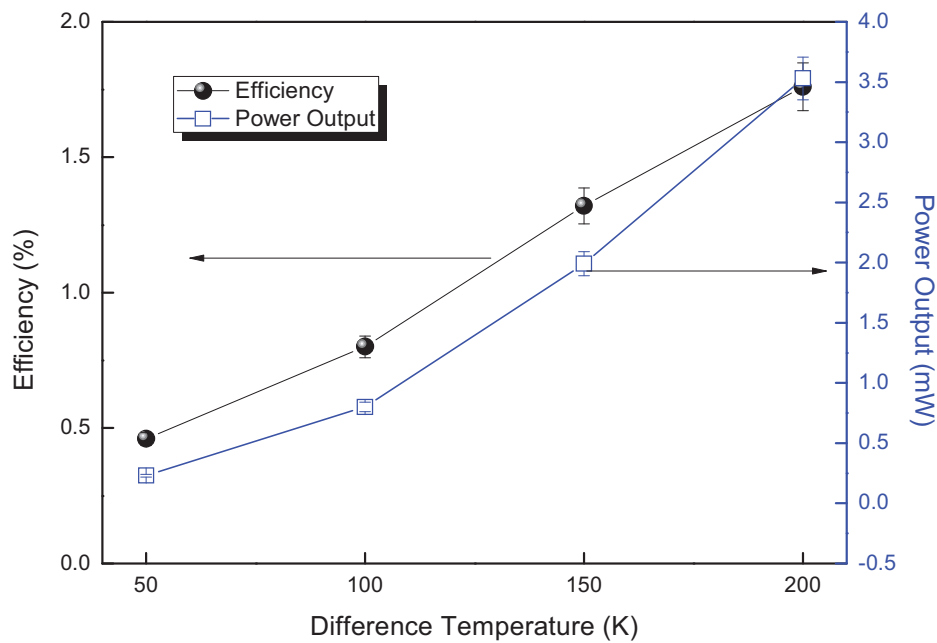


**Figure 8.** The result of simulation of power output, efficiency at difference temperature ranging from 50–200 K.



is 0.22 mW. The distributions of temperatures for thermoelectric on FEM 17 cell and distributions of voltage for thermoelectric FEM cell under different operating conditions as shown in Fig. 6.

Figure 7 shows the voltage and electrical current produced by TEG 17 cells rise sharply to the maximum of 0.92 V and 3.68 mA, respectively. The difference temperature across the TEG is now 200 K, which is obtained from the generation characteristic of TEG. Fig. 8 shows the power output and efficiency of each cell rise with increasing difference temperature from 200 K the efficiency from 1.76 % and the power output from 3.53 mW. This result showed that the thermoelectric 17 cells higher than thermoelectric 1 cell. However, the electric current of thermoelectric 17 cells has been lower than thermoelectric 1 cell.

## 6. Conclusions

This paper presents the results of numerical simulation thermoelectric cell through the use of finite element method. The simulation findings also based on the FEM analysis revealed the Seebeck coefficient resistivity and thermal conductivity of the material thermoelectric p-type sodium cobalt oxide doping silver (NaCo<sub>2</sub>O<sub>4</sub>/Ag) and the n-type calcium bismuth manganese oxide (CaMnO<sub>3</sub>/Bi) of size  $2.5 \times 2.5 \times 10 \text{ mm}^3$ . The was placed on a  $2.5 \times 5.5 \times 0.5 \text{ mm}^3$  copper plate in order to analyze the performance of thermoelectric, temperature distribution, heat flux, power output, voltage and electrical current. Efficiency of the thermoelectric cell of 1&17 cells increased from 0.11 % and 1.76 % respectively, at temperature difference 200 K.

## Funding

Financial supported by Graduate School Sakon Nakhon Rajabhat University Thermoelectrics Research Center and National Electronics and Computer Technology Center.

## Nomenclature

$E$	electric field ( $\text{N C}^{-1}$ )
$I$	electric current density ( $\text{A m}^{-2}$ )
$J_{\max}$	maximum current density ( $\text{A m}^{-2}$ )
$R_L$	load resistance ( $\Omega$ )
$R_{TEG}$	TEG electrical resistance ( $\Omega$ )
$T_C$	heat sink temperature (K)
$T_H$	heat source temperature (K)
$A$	cross-sectional area of p-type and n-type TEG thermo elements ( $\text{m}^2$ )
$Q$	thermal input (W)
$P$	power output (W)
$V$	voltage (V)

## References

1. S. Priya and D. J. Inman, *Energy harvesting technologies*. Boston (MA) Springer; 2009.
2. ANSYS®. *Academic Research, Release 13.0, Help System, Coupled Field Analysis Guide*, ANSYS, Inc; 2010.
3. S. Angrist, 3rd Edition, *Allyn and Bacon Boston Dynamics* 1976; 140–166.

4. L. D. Landau, and E. M. Lifshitz, *Electrodynamics of Continuous Media*. 2nd Edition, Butterworth-Heinemann Oxford; 1984.
5. C. Min, A. R. Lasse, and C. Thomas, A three-dimensional numerical model of thermoelectric generators in fluid power systems. *International J. Heat and Mass. Transfer* **54**, 345–355 (2011).
6. D. Yuan, Z. Wei, W. Yao, and S. Yongming, Enhanced performance of solar-driven photovoltaic—thermoelectric hybrid system in an integrated design. *J. Solar. Energy* **88**, 182–191 (2013).
7. X. Jinsheng, Y. Tianqi, L. Peng, Z. Pengcheng, and Z. Qingjie, Thermal design and management for performance optimization of solar thermoelectric generator. *J. Applied Energy* **93**, 33–38 (2012).
8. P. P. Silvester and R. L. Ferrari, *Finite Elements for Electrical Engineers*. 3rd Edition, University Press Cambridge; 1996.